

# THESIS

## Study of Decay of Correlations in a System of Two Falling Balls

Gábor Borbély

**Supervisor:** Péter Bálint Dr.  
associate professor  
BME Institute of Mathematics,  
Department of Differential Equations

**BME**  
**2010**

# Contents

<b>1</b>	<b>Introduction and Historical Overview</b>	<b>1</b>
1.1	Stochastic Properties . . . . .	1
1.2	Motivation for Billiards . . . . .	4
<b>2</b>	<b>System of two Falling Balls</b>	<b>6</b>
2.1	Expressing the Dynamics Explicitly . . . . .	7
2.2	Properties of $D F_1$ and $D F_2$ . . . . .	9
2.2.1	KAM phenomena . . . . .	10
2.3	Hyperbolicity . . . . .	11
2.3.1	Cones . . . . .	13
2.4	The First Return Map and the Singularity Stripes . . . . .	16
<b>3</b>	<b>Analysis of the First Return Sets</b>	<b>19</b>
3.1	Bounding Functions . . . . .	20
3.2	A Simplified Model . . . . .	22
3.3	Straightening the Stripes . . . . .	25
3.4	Summary . . . . .	28
<b>4</b>	<b>Afterword</b>	<b>30</b>

# Chapter 1

## Introduction and Historical Overview

In the most general sense this thesis is on the field of study of dynamical systems. In mathematics a physical system is represented as a map  $T : M \mapsto M$  where the set  $M$  is the phase space. In discrete time the map  $T$  acts the system one step forward, in continuous time  $T_t$  depends on a parameter  $t \in I$ , where  $I \subseteq \mathbb{R}$  is a specified interval. The flow  $T_t$  evolves the system  $t$  time forward and  $T_{t+s} = T_t \circ T_s$ . If the system is at the state  $x \in M$  at the time 0, then it will be in the state  $T_t x$  at the time  $t$ .

### 1.1 Stochastic Properties

Sometimes it is not useful or interesting to study the smaller details of a system (motion) but one asks questions like: Where is a particle after a long time? What pattern can I see when I start the system from a typical configuration and look at it after a long time?

This type of approach can be familiar for example from the statistical physics. To ensure that the above questions make sense we have to study certain stochastic properties.

Ergodic theory studies the behavior of dynamical systems in the above mentioned way and it's main interest is the evolution of measures.

**Definition 1.1.1** *Take a phase space:  $\mathcal{M}$  and a dynamics (in discrete time):  $T : \mathcal{M} \mapsto \mathcal{M}$ .  $T$  is an endomorphism on the probability measure space  $(\mathcal{M}, \Sigma, \mu)$  if  $T$*

preserves  $\mu$ .

$$\begin{aligned} \mu(\mathcal{M}) &= 1 & \text{and} \\ \mu(T^{-1}A) &= \mu(A) & \text{for every } A \in \Sigma \end{aligned}$$

If  $T$  is invertible and  $T^{-1}$  is also an endomorphism with  $\mu$  then we call it an automorphism and  $\mu(TA) = \mu(A)$  also holds. An endomorphism  $T : \mathcal{M} \mapsto \mathcal{M}$  with a measure  $\mu$  means the objects together:  $(T, \mathcal{M}, \Sigma, \mu)$

The most basic property is the ergodicity.

**Definition 1.1.2** A  $T : \mathcal{M} \mapsto \mathcal{M}$  endomorphism with a measure  $\mu$  is ergodic if: every invariant  $f : \mathcal{M} \mapsto \mathbb{R}$  function is constants almost everywhere.

$$\mu(\{x \in \mathcal{M} | f(x) = f(Tx)\}) = 1 \Rightarrow \mu(\{x \in \mathcal{M} | f(x) = c\}) = 1$$

For some  $c \in \mathbb{R}$ .

The existence of a nontrivial invariant set disproves ergodicity. If the set  $A \subseteq \mathcal{M}$  is invariant ( $\mu(A \Delta T^{-1}A) = 0$ ) and  $0 < \mu(A) < 1$  then the function  $\mathbb{I}_{\{x \in A\}}$  is invariant however not constant almost everywhere. The lack of a nontrivial invariant set is also an equivalent characterization of ergodicity [13].

In the definition 1.1.2 the function  $f : \mathcal{M} \mapsto \mathbb{R}$  can be regarded as a measurement. In physics this means that we measure a certain quantity ( $f(x) \in \mathbb{R}$ ) in a certain state of the system ( $x \in \mathcal{M}$ ). Sometimes the function  $f : \mathcal{M} \mapsto \mathbb{R}$  is called an *observable*. In the terminology of probability theory we think of an observable of an endomorphism as a random variable in the following way: let  $(\mathcal{M}, \Sigma, \mu)$  be a probability space of an endomorphism and  $f : \mathcal{M} \mapsto \mathbb{R}$  a  $\mu$ -measurable function.

**Definition 1.1.3** Let  $(T, \mathcal{M}, \Sigma, \mu)$  be an endomorphism and  $f \in L^1_\mu(\mathcal{M})$  be an observable. The space average of  $f$  is:

$$\mathbb{E}(f) := \int_{\mathcal{M}} f(x) \, d\mu(x)$$

The time average of  $f$  is:

$$\begin{aligned} \hat{f} &:= \lim_{n \rightarrow \infty} \frac{1}{n} \sum_{i=0}^{n-1} f \circ T^i \\ \hat{f}(x) &= \lim_{n \rightarrow \infty} \frac{f(x) + f(Tx) + \dots + f(T^{n-1}x)}{n} \end{aligned}$$

If the limit exists.

We call  $(S_n f)(x) = f(x) + f(Tx) + \dots + f(T^{n-1}x)$  the *Birkhoff sum* of  $f$ .

One can easily check that  $\hat{f}$  is invariant (if it exists). Therefore in ergodic endomorphisms the  $\hat{f}$  is constant almost everywhere.

The following theorem is the equivalent of Law of Large Numbers in Ergodic theory.

**Theorem 1.1.4 (Birkhoff)** *Let  $(T, \mathcal{M}, \Sigma, \mu)$  be an endomorphism and  $f \in L^1_\mu(\mathcal{M})$  an observable.*

*If the  $T$  is ergodic then the time average does exist almost everywhere and*

$$\hat{f} = \mathbb{E}(f) \quad \text{almost everywhere.}$$

*In other words the time average converges to the space average (for  $\mu$ -typical points).*

*Mixing* is a stronger stochastic property than ergodicity, it is motivated by the independence (uncorrelatedness) of random variables.

**Definition 1.1.5** *A  $T : \mathcal{M} \mapsto \mathcal{M}$  endomorphism with a measure  $\mu$  is mixing if: for any measurable  $A, B \subseteq \mathcal{M}$*

$$\lim_{n \rightarrow \infty} \mu(T^{-n}A \cap B) = \mu(A)\mu(B)$$

Another definition:

**Definition 1.1.6** *A  $T : \mathcal{M} \mapsto \mathcal{M}$  endomorphism with a measure  $\mu$  is mixing if: for any square-integrable functions  $f, g \in L^2_\mu(\mathcal{M})$*

$$\begin{aligned} \lim_{n \rightarrow \infty} \mathbb{E}((f \circ T^n)g) &= \mathbb{E}(f)\mathbb{E}(g) \quad \text{that is} \\ \lim_{n \rightarrow \infty} \int_{\mathcal{M}} f(T^n x)g(x) \, d\mu(x) &= \int_{\mathcal{M}} f(x) \, d\mu(x) \int_{\mathcal{M}} g(x) \, d\mu(x) \end{aligned}$$

If  $f, g$  are indicator functions of measurable sets, then this formula is the same as in definition 1.1.5. In [13] one can see the equivalence of these two definitions. The latter definition allows to define the *decay of correlations* for specific observables. Motivated by the subject of our study I use more specific conditions on the below introduced objects, and through at the thesis. From now on I assume that the phase space is always a Riemannian manifold.

**Definition 1.1.7** *A  $T$  endomorphism on a Riemannian manifold  $\mathcal{M}$  with a Borel measure  $\mu$  mixes with a polynomial rate  $\alpha \geq 0$  if:*

*for any Hölder continuous functions  $f, g : \mathcal{M} \mapsto \mathbb{R}$*

*there exists a  $c \geq 0$  such that the following holds (for every  $n \in \mathbb{N}$ )*

$$|\mathbb{E}((f \circ T^n)g) - \mathbb{E}(f)\mathbb{E}(g)| \leq cn^{-\alpha}$$

In the definition  $\mathcal{M}$  does not have to be a Riemannian manifold but it has to be a metric space in order to define Hölder continuity. Meanwhile  $\mathcal{M}$ , in the examples of physics, is usually a Riemannian manifold.

To define an *exponential rate of mixing* we use  $c\lambda_{f,g}^n$  as a bound where  $\lambda_{f,g}$  depends on the Hölder exponents of  $f$  and  $g$ .

Since the Law of Large Numbers holds for every ergodic endomorphism it is natural to study the CLT.

**Definition 1.1.8** *For an ergodic endomorphism  $(T, \mathcal{M}, \Sigma, \mu)$  the Central Limit Theorem holds if:*

*for any Hölder continuous function  $f : \mathcal{M} \mapsto \mathbb{R}$*

$$\lim_{n \rightarrow \infty} \mu \left( \frac{S_n f}{\sqrt{n}\sigma} \leq z \right) = \frac{1}{\sqrt{2\pi}} \int_{-\infty}^z e^{-\frac{x^2}{2}} dx$$

*Where  $f$  is supposed to be "centered":  $\mathbb{E}(f) = 0$*

*and  $\sigma$  is the "variance".*

$$\sigma_f^2 = \sum_{n=-\infty}^{\infty} \mathbb{E}(f(f \circ T^n))$$

Here one can see that the fast decay of correlations is crucial in CLT. Without the series  $\sum_n \mathbb{E}(f(f \circ T^n))$  being summable there is no chance to have CLT.

These (and further) properties were discussed in many systems. In systems with strong stochastic properties a typical trajectory cannot be distinguished from realizations of random processes. One crucial point of these discussions is the decay of correlations and the purpose of this thesis is to study this property for the system of two falling balls.

## 1.2 Motivation for Billiards

Billiards are special dynamical systems. Let a point particle move freely in a bounded domain (billiard table)  $Q$ , usually  $Q$  is in Euclidean space or on a torus. The boundary  $\partial Q$  is piecewise smooth. The particle reflects from the boundary according to the law of specular reflection (angle of incidence equals angle of reflection). Thus billiard orbits are broken lines and the kinetic energy of the particle is an integral of motion. The speed of the ball is assumed to be 1.

Billiards on two dimensional tables are quite in the focus of the current interest. The behaviour of such a system is strongly determined by the shape of  $\partial Q$ . If the table is a circle or a rectangle, then the system is integrable (for a definition see [1]). If the boundary is piecewise concave (centers of curvature lie outside of  $Q$ ), then the system has strong chaotic properties. This kind of billiards are called Sinai

billiards, see [12]. Chernov proved advanced stochastic properties in Sinai billiards [5] (e.g. strong versions of the CLT).

If the table has (partly) convex boundary then one could suspect that the system does not have stochastic properties, since the wall of the table does not scatter the trajectories, but focuses them. However one can construct ergodic, convex billiard tables, the best known examples are stadia ([4]). In stadium billiards the CLT typically does not hold. There is an equivalent condition for CLT in [2].

There are several possible ways to generalize billiard systems. For example with  $n$  particle with various mass ratios. In this case the particles have a non-zero volume (radius) to ensure that they collide with non-zero probability. This system is the hard sphere gas model. [10] [14]

An other way of generalization is to place the table in an external field and give charge to the particle, this way the inter-collisional trajectories are no longer straight line segments. [7] [8] [15]

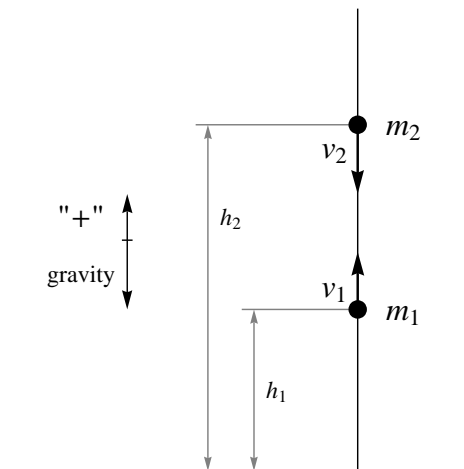
The below introduced system is also a much-discussed type of billiards.

# Chapter 2

## System of two Falling Balls

The system of falling balls can be regarded as a billiard. The table is one dimensional: a vertical half line bounded from below. In this line infinitesimally small balls move up and down under the force of gravity ( $g$  traditionally denotes  $9.81 \frac{m}{s^2}$ ). They bounce and collide totally elastically with each other and with the floor. Our system has only two particles of mass  $m_1$  and  $m_2$ .

Figure 2.1:



Wojtkowski in [16] studied a general case: a system of  $n$  balls with different masses  $m_n$ . He proved hyperbolicity (see the definition in section 2.3) if the masses do not increase up the line and none of them are equal.

$$m_1 > m_2 > \dots > m_n$$

In [11] the hyperbolicity is proved under a weaker assumption.

From [9] we know that the system of two balls is ergodic in the case in which the lower ball is heavier ( $m_1 > m_2$ ). This case is the main subject of this thesis. The second case is when the  $m_1 = m_2$ . In this case the balls exchange velocity which



makes the system completely integrable. The third case is when  $m_1 < m_2$ . I will refer to this case in section 2.2.1.

## 2.1 Expressing the Dynamics Explicitly

We neglect the air resistance therefore the total energy of the system  $J := \frac{1}{2}m_1v_1^2 + m_1gh_1 + \frac{1}{2}m_2v_2^2 + m_2gh_2$  is an integral of motion. This motivates introducing the phase space  $\hat{\mathcal{M}}$ :

$$\left\{ (h_1, v_1, h_2, v_2) \in \mathbb{R}^4 \mid h_1 > 0, h_2 > 0, \frac{1}{2}m_1v_1^2 + m_1gh_1 + \frac{1}{2}m_2v_2^2 + m_2gh_2 = J \right\}$$

The dynamics act on  $\hat{\mathcal{M}}$  in continuous time. In order to use our notations it is useful to discretize the system. Like Wojtkowski did in [16] we introduce the Poincaré section  $\mathcal{M} = \left\{ (h_1, v_1, h_2, v_2) \in \hat{\mathcal{M}} \mid h_1 = 0, v_1 > 0 \right\}$ . This means that we consider the moments when the lower ball hits the floor infinitesimally after the collision. Now we have a discrete map of a two dimensional phase space  $T : \mathcal{M} \mapsto \mathcal{M}$ . In the rest of my thesis I will try to understand the properties of this single map.

Instead of the usual moments we use the following coordinates of  $\mathcal{M}$  (also from [16]):

$$h := \frac{1}{2}m_1v_1^2 \quad \text{the total energy of the lower ball, since } h_1 = 0$$

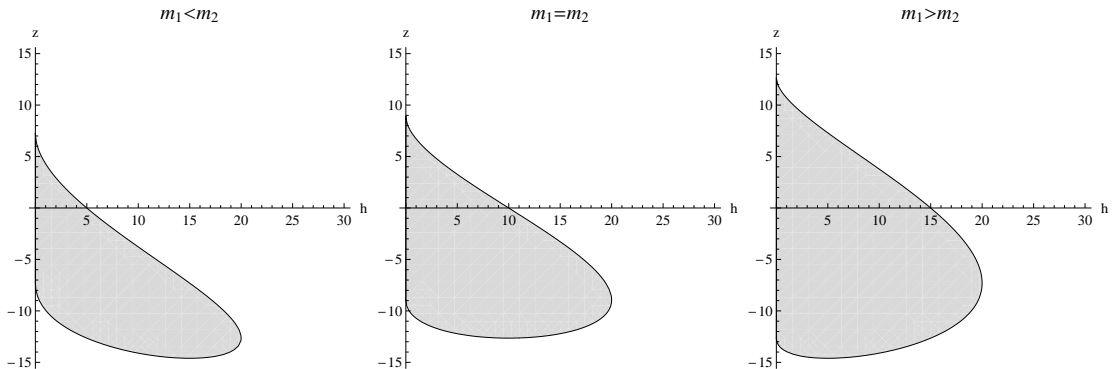
$$z := v_2 - v_1$$

These coordinates seem to be suitable because they make our formulas simpler. It is also interesting to see that these quantities are invariants during the inter-collisional motion. Now the phase space is the following:

$$\mathcal{M} := \left\{ (h, z) \in \mathbb{R}^2 \mid (0 < h < J) \wedge \left( J - h > \frac{1}{2}m_2v_2^2 \right) \right\}$$

Where  $v_2$  can be expressed from our coordinates:  $v_2 = v_1 + z = \sqrt{\frac{2h}{m_1}} + z$

Figure 2.2: The phase space for different masses with  $J = 20$



Notice that  $T$  is only piecewise continuous. Considering the collisions there are two cases: when the two balls collide before the lower one returns to the floor and the opposite.

$$\mathcal{M} \supseteq \mathcal{M}_1 = \{\text{configurations in which the balls will collide}\}$$

$$\mathcal{M} \supseteq \mathcal{M}_2 = \{\text{configurations in which the balls won't collide}\}$$

$$(h', z') = T(h, z) = \begin{cases} F_1(h, z) & \text{if } (h, z) \in \mathcal{M}_1 \\ F_2(h, z) & \text{if } (h, z) \in \mathcal{M}_2 \end{cases}$$

I denoted the action of  $T$  by prime.

With these notations  $F_i$  is a smooth  $\mathcal{M}_i \mapsto \mathcal{M}$  map. To determine the sets  $\mathcal{M}_i$  pretend for a while that the two balls move independently. To fall back to the floor the lower ball would take  $t = 2\frac{v_1}{g}$  time, meanwhile the upper ball would reach the height  $h_t = h_0 + v_2 t - \frac{1}{2}gt^2$  where  $h_0$  is the starting height, which can be calculated from the potential energy of the upper ball:  $h_0 = \frac{J - h - \frac{1}{2}m_2 v_2^2}{gm_2}$ . After the substitutions:

$$h_t = \frac{m_2 m_1 z \left( 2\sqrt{\frac{2h}{m_1}} - z \right) - 2h(m_1 + m_2) + 2Jm_1}{2gm_1 m_2} \quad (2.1)$$

I used Wolfram Mathematica for the substitution and also in the further calculations therefore they are not detailed.

Whether the balls collide or not is determined by the sign of  $h_t$ . Now the sets can be determined:

$$\mathcal{M}_1 := \{(h, z) \in \mathcal{M} | h_t < 0\}$$

$$\mathcal{M}_2 := \{(h, z) \in \mathcal{M} | h_t > 0\}$$

We do not consider the case  $h_t = 0$  because it is an event with zero probability and no matter how we define the map  $T$  in this non-typical case, it does not effect the statistical properties of the system. Surprisingly, even though the gravity force appears in the formula (2.1), it does not effect the sign of it.

Now we can determine the maps  $F_i$ , starting with the easier case of  $F_2$ , when the balls do not collide. As the individual energies are conserved  $h' = h$  and consequently  $v_1' = v_1$ . Since the balls accelerate equally  $v_2' = v_2 - 2v_1$  and  $z' = v_2' - v_1' = (v_2 - 2v_1) - v_1 = z - 2v_1$ .

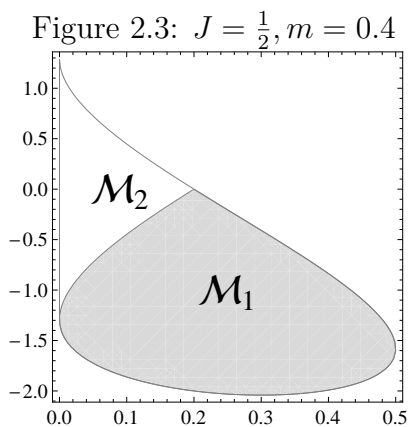
$$\begin{pmatrix} h' \\ z' \end{pmatrix} = F_2(h, z) = \begin{pmatrix} h \\ z - 2v_1 \end{pmatrix} = \begin{pmatrix} h \\ z - 2\sqrt{\frac{2h}{m_1}} \end{pmatrix}$$

To determine  $F_1$  one has to express the following quantities in the terms of  $h$  and  $z$ . The time when the particles reach the same height (and also the height itself), count the velocities in that moment, apply the rules of an elastic collision and calculate the additional time needed for the lower particle to hit the floor again. The values of  $h'$  and  $z'$  can be determined from the new velocities and kinetic energies. This calculation results the formula (2.2). For simplicity we make the assumption:  $m_1 + m_2 = 1$  because these parameters only scale the system. From now on let  $m_1 = m$  and  $m_2 = 1 - m$  where  $0 < m < 1$ . Also  $J$  is often assumed to be  $\frac{1}{2}$ .

$$\begin{pmatrix} h' \\ z' \end{pmatrix} = F_1(h, z) = \begin{pmatrix} m(2J + (2m^2 - 3m + 1)z^2) - h \\ 2\sqrt{2}\sqrt{-\frac{h}{m} + 2J + (2m^2 - 3m + 1)z^2} - z \end{pmatrix} \quad (2.2)$$

It is interesting to notice that the gravity force does not occur in any of the formulas. Finally let's define the dynamics.

$$T(h, z) := \begin{cases} F_1(h, z) & \text{if } (h, z) \in \mathcal{M}_1 \\ F_2(h, z) & \text{if } (h, z) \in \mathcal{M}_2 \end{cases}$$



## 2.2 Properties of $D F_1$ and $D F_2$

The Jacobian of the maps can be calculated:

$$D F_1(h, z) = \begin{pmatrix} -1 & 2m\alpha z \\ \frac{\sqrt{2}}{m\sqrt{1-\frac{h}{m}+\alpha z^2}} & -1 - \frac{2\sqrt{2}m\alpha z}{\sqrt{1-\frac{h}{m}+\alpha z^2}} \end{pmatrix}$$

$$D F_2(h, z) = \begin{pmatrix} 1 & 0 \\ -\sqrt{\frac{1}{2hm}} & 1 \end{pmatrix}$$

Where  $\alpha := m_2(m_2 - m_1) = (1 - m)((1 - m) - m) = 1 - 3m + 2m^2$ . The sign of  $\alpha$  plays an important role because, as I mentioned in section 2.1, it characterizes the behavior of the system.  $\alpha$  is determined by the mass ratio of the balls: if  $m_1 > m_2$  then  $\alpha < 0$ , if  $m_1 = m_2$ , then  $\alpha = 0$ , otherwise  $\alpha > 0$ . We are interested in the case of negative  $\alpha$  because this corresponds to ergodic dynamics.

As you look at the matrices  $D F_1$  and  $D F_2$  you can see that the *Lebesgue measure* is preserved by the map  $T$  because both matrices have determinant 1. So the map  $T$  with the normalized Lebesgue measure on  $\mathcal{M}$  (denoted by  $\mu := \frac{\lambda}{\lambda(\mathcal{M})}$ ) is an endomorphism. (Actually, it is an automorphism but we do not see this now)

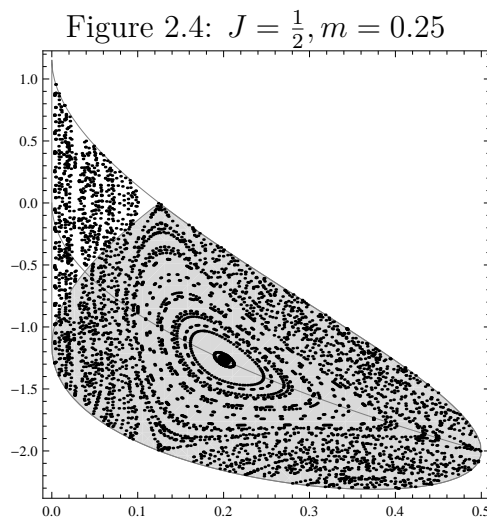
## 2.2.1 KAM phenomena

Why aren't we interested in  $\alpha > 0$ ? Wojtkowski showed in [16] that in the case  $\alpha > 0$  there exists a stable fixed point. You can find a fixed point as a solution of the system of equations:

$$F_1(h, z) = \begin{pmatrix} h \\ z \end{pmatrix}$$

The solution  $\left(\frac{J}{3-2m}, -\sqrt{\frac{2J}{m(3-2m)}}\right)$  lies in  $\mathcal{M}_1$ , the region where you have to apply  $F_1$  and at this point  $D F_1$  is an elliptic matrix (if  $\alpha > 0$  then the Jacobian at the same point is hyperbolic). Unless some resonances take place, the existence of a stable fixed point implies the existence of a non-trivial invariant set in  $\mathcal{M}$ , which would disprove the ergodicity.

It would be interesting to study these KAM phenomena but they are out of the framework of chaotic behaviour. In [13] and [1] one can read more about these phenomena. Figure 2.4 shows 61 randomly chosen points and their trajectories for



80 iterations. The big point in the middle is the stable fixed point.

## 2.3 Hyperbolicity

To introduce Lyapunov exponents first we consider linear maps. Take a two dimensional square matrix:  $A$ . Suppose that  $A$  has two different eigenvalues:  $\lambda_1, \lambda_2$ , and the corresponding eigenvectors are:  $u_1, u_2$ . Then  $A$  acts on  $u_i$  as:

$$\begin{aligned} A^n u_i &= \lambda_i^n u_i \\ \|A^n u_i\| &= |\lambda_i|^n \|u_i\| \\ \log \|A^n u_i\| &= n \log |\lambda_i| + \log \|u_i\| \\ \frac{1}{n} \log \|A^n u_i\| &= \log |\lambda_i| + \frac{\log \|u_i\|}{n} \\ \lim_{n \rightarrow \infty} \frac{1}{n} \log \|A^n u_i\| &= \log |\lambda_i| \end{aligned}$$

So the eigenvector grows or shrinks exponentially fast depending on the sign of  $\log |\lambda_i|$ . In this case the Lyapunov exponents are the log-eigenvalues. In a general case we have a smooth ( $C^1$ ) map acting on a smooth manifold:  $T : \mathcal{M} \mapsto \mathcal{M}$ . Take a point  $x \in \mathcal{M}$  and a vector in the tangent space:  $v \in \mathcal{T}_x \mathcal{M}$ .  $T$  acts on a pair  $(x, v)$  in a natural way:  $T(x, v) = (Tx, DT_x \cdot v)$

**Definition 2.3.1** A point  $x$  HAS a Lyapunov exponent:  $\chi$  and a characteristic subspace:

$\mathcal{E}_x^\chi \subseteq \mathcal{T}_x \mathcal{M}$  if:

For every  $v \in \mathcal{E}_x^\chi$

$$\lim_{n \rightarrow \infty} \frac{1}{n} \log \|T^n(x, v)\| = \chi$$

The existence of these objects is not guaranteed. The Oseledec theorem, see [4], states that the exponents exist almost everywhere, with respect to any invariant measure, if the  $T$  is differentiable on the phase space. The exponents also exist if the endomorphism satisfies some weaker properties, also mentioned in [4]. In [16] one can see that those conditions are fulfilled by our system: piecewise smoothness, and some non-degeneracy conditions for  $T$ .

If  $\chi < 0$  we call  $\mathcal{E}_x^\chi$  a stable subspace of  $x$ , if  $\chi > 0$  an unstable subspace, otherwise neutral. The vectors in a stable subspace shrink exponentially fast as  $n \rightarrow \infty$  and grow exponentially fast as  $n \rightarrow -\infty$ . The vectors in an unstable subspace act vice verse. If we consider a higher dimensioned manifold and there are more exponents:  $\chi_1, \chi_2, \dots, \chi_m$  with the corresponding subspaces:  $\mathcal{E}_x^{\chi_1}, \mathcal{E}_x^{\chi_2}, \dots, \mathcal{E}_x^{\chi_m}$  then we group the subspaces according to the sign of the exponents. This way we have three subspaces for every point:

$$\mathbb{R}^n \cong \mathcal{T}_x \mathcal{M} = \underbrace{\left( \bigoplus_{\chi_i < 0} \mathcal{E}_x^{\chi_i} \right)}_{\mathcal{E}_x^s} \oplus \underbrace{\left( \bigoplus_{\chi_i > 0} \mathcal{E}_x^{\chi_i} \right)}_{\mathcal{E}_x^u} \oplus \underbrace{\left( \bigoplus_{\chi_i = 0} \mathcal{E}_x^{\chi_i} \right)}_{\mathcal{E}_x^n}$$

**Definition 2.3.2** A map  $T$  acting on a Riemannian manifold  $\mathcal{M}$  is hyperbolic if  $\mathcal{E}_x^n$  is trivial but none of the  $\mathcal{E}_x^s, \mathcal{E}_x^u$  are trivial (and do exist) for almost every point with respect to the Lebesgue measure.

Notice that in our system the Lebesgue measure, on the manifold  $\mathcal{M}$ , is itself an invariant measure. In general it can happen that the invariant measure is singular. However a system can be hyperbolic in the above sense without a Lebesgue-continuous invariant measure.

In a two dimensional map the hyperbolicity means that there is one stable and one unstable direction in the Lebesgue-typical points. The directions of the (un)stable subspaces determine a vector field in the phase space. The integral curves through these directions are the (un)stable manifolds. It is easy to determine these manifolds and exponents if the map is linear. For example in the CAT map (discussed in [13]) one has to calculate the eigendecomposition of the CAT matrix. But this is a more difficult task in a general case.

How can we determine the exponents from  $D F_1$  and  $D F_2$ ? Suppose that almost every point has a negative (stable) Lyapunov exponent:  $\chi_x$ . Then the function  $f : x \mapsto \chi_x$  is an invariant function since the trajectory of a point  $x$  overlaps with the trajectory of  $Tx$  (except in one point:  $x$ ). Hence the asymptotic behaviour is the same for  $x$  and  $Tx$ . By ergodicity this function should be constant almost everywhere, therefore the system has ONE stable Lyapunov exponent  $\chi$ .

Take the "one-step" Lyapunov exponents:  $g : x \mapsto \log |\lambda_x|$ , the log-eigenvalues of  $D F_1$  or  $D F_2$  (take the eigenvalue  $|\lambda_x| < 1$ ). The time average of this function gives exactly the asymptotic expansion rate of a vector in the stable subspace.

$$\lim_{n \rightarrow \infty} \frac{\log |\lambda_x| + \log |\lambda_{Tx}| + \dots + \log |\lambda_{T^{n-1}x}|}{n} = \lim_{n \rightarrow \infty} \frac{\log |\lambda_x \lambda_{Tx} \dots \lambda_{T^{n-1}x}|}{n} = \hat{g}(x)$$

And we know from the Birkhoff ergodic theorem that

$$\int_{\mathcal{M}} g(x) d\mu(x) = \int_{\mathcal{M}} \underbrace{\hat{g}(x)}_{\text{constant}} d\mu(x) = \chi \int_{\mathcal{M}} d\mu(x) = \chi$$

Take a  $2 \times 2$  matrix with determinant 1 and denote the magnitude of the smaller eigenvalue with  $|\text{eig}(A)| \leq 1$ . In our system with this notation

$$\begin{aligned} \chi &= \int_{\mathcal{M}} \log |\text{eig}(D_x T)| d\mu(x) = \\ &= \frac{1}{\lambda(\mathcal{M})} \left( \int_{\mathcal{M}_1} \log |\text{eig}(D F_1(h, z))| dh dz + \int_{\mathcal{M}_2} \log \overbrace{|\text{eig}(D F_2(h, z))|}^1 dh dz \right) = \\ &= \frac{1}{\lambda(\mathcal{M})} \int_{\mathcal{M}_1} \log |\text{eig}(D F_1(h, z))| dh dz \end{aligned}$$

The unstable exponent of the system is  $-\chi$  because the matrices  $D F_1, D F_2$  have determinant 1.

$$\int_{\mathcal{M}} \log \overbrace{\left| \frac{1}{\text{eig}(D_x T)} \right|}^{\text{the other eigenvalue}} d\mu(x) =$$

$$\int_{\mathcal{M}} -\log |\text{eig}(D_x T)| d\mu(x) = -\chi$$

This integral seems impossible to calculate but I could calculate the exponent numerically, for a fixed  $m$ . Figure 2.9 represents the values of  $\chi$  for different mass ratios.

There is a numerical method to visualize the unstable subspaces too but first we have to define cones.

### 2.3.1 Cones

**Definition 2.3.3** *In a linear space  $A$  a cone  $\mathcal{C}$  is a subset of  $A$  which is closed under the scalar multiplication. (a collection of directions)*

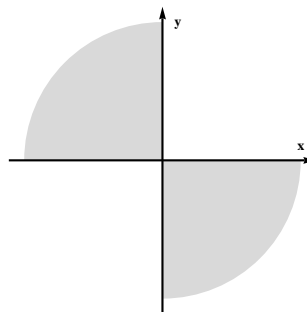
$$x \in \overbrace{\mathcal{C}}^{\subseteq A} \Rightarrow \lambda x \in \mathcal{C} \quad \forall \lambda \in \mathbb{R}$$

*In a Riemannian manifold  $R$  a cone in a point  $x \in R$  is subset of the tangent space  $\mathcal{C}_x \subseteq \mathcal{T}_x R$  which is a cone in  $\mathcal{T}_x R$ .*

A special way of defining cones (in a point of a Riemannian manifold  $R$ ) is to take two vectors  $v_1, v_2 \in \mathcal{T}_x R$  and let

$$\mathcal{C}_x(v_1, v_2) = \pm\{\alpha_1 v_1 + \alpha_2 v_2 \mid \alpha_1 \geq 0 \text{ and } \alpha_2 \geq 0\} \subseteq \mathcal{T}_x R$$

Figure 2.5:



**Definition 2.3.4** A cone field, of a Riemannian manifold  $R$ , is a set of cones  $\{\mathcal{C}_x\}_{x \in R}$ . We require continuity in the following sense.

To compare two cone we need a metric:  $d(\mathcal{C}_x, \mathcal{C}_y)$ . Since we have a Riemannian manifold we can compare sets in tangent spaces of nearby points by identifying the tangent spaces with parallel translation. To compare sets in the same tangent space we take the unit vectors in a cone:

$$\mathcal{C}_x^1 = \{v \in \mathcal{C}_x : |v| = 1\}$$

and use the Hausdorff metric:  $d_H(\mathcal{C}_x^1, \mathcal{C}_y^1)$

We will deal only with cones given by a pair of vectors and in this case the continuity is easier to define.

In our case  $R = \mathcal{M} \subseteq \mathbb{R}^2$ . To simplify the formalism of cones we identify the tangent spaces  $\mathcal{T}_x \mathcal{M} \cong \mathbb{R}^2$  with the same  $\mathbb{R}^2$  in which  $\mathcal{M}$  is embedded. A cone field in our case is the following.

$$\{\mathcal{C}_x(v_1(x), v_2(x))\}_{x \in \mathcal{M}}$$

Where  $v_i : \mathcal{M} \mapsto \mathbb{R}^2$  are continuous functions determining the sides of the cones.

**Definition 2.3.5** Let  $T : \mathcal{M} \mapsto \mathcal{M}$  be our endomorphism. A cone field  $\{\mathcal{C}_x\}_{x \in \mathcal{M}}$  is invariant if  $T$  maps every cone inside the cone at the image point.

$$D T_x(\mathcal{C}_x) \subseteq \mathcal{C}_{T_x} \quad \text{for almost every } x \in \mathcal{M}$$

In the definition  $T$  acts on a cone  $\mathcal{C}_x \subseteq \mathcal{T}_x \mathcal{M}$  in a natural way: represent a cone with vectors from all of the directions and apply  $D T_x$  for all of them.  $\{D T_x \cdot v\}_{v \in \mathcal{C}_x}$  can be obtained as an other collection of directions in  $\mathcal{T}_{T_x} \mathcal{M}$ .

In the following section we will prove that the following (constant) cone field is invariant with respect to our system.

$$\{\mathcal{C}_x(e_1, -e_2)\}_{x \in \mathcal{M}} \quad \text{where } e_i \text{ are the standard basis vectors in } \mathbb{R}^2$$

Note that  $A = \mathcal{C}_x(e_1, -e_2)$  is the union of the lower, right quarter and the upper, left quarter of the plane.

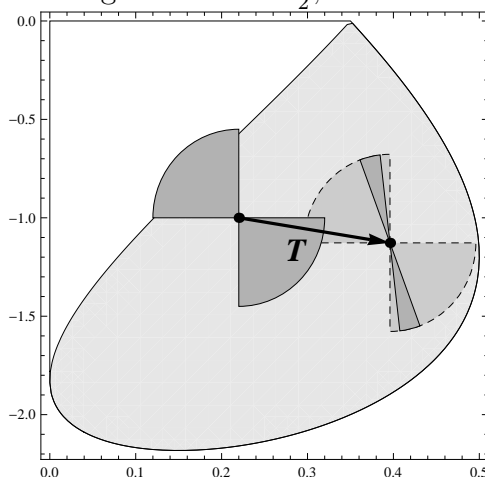
Let  $\underline{x} = (x, y) \in A$  be a vector in the cone. We check the invariance for both  $F_1$ , and  $F_2$ . Let us consider  $F_1$  first ( $(h, z) \in \mathcal{M}_1$ ):

$$D F_1 \cdot \underline{x} = \begin{pmatrix} 2myz\alpha - x \\ \frac{\sqrt{2}(x-2myz\alpha)}{m\sqrt{-\frac{h}{m}+z^2\alpha+1}} - y \end{pmatrix}$$

Notice that  $\alpha < 0$  (ergodic case) and we will show with an indirect reasoning that  $z < 0$ . Assume the contrary, as the balls do collide ( $D F_1$  should act on  $\underline{x}$ ) and



Figure 2.6:  $J = \frac{1}{2}, m = 0.7$



$z$  is positive then  $z > 0$  should also hold in the moment infinitesimally before the collision, since  $z$  is an integral of inter-collisional motion. But  $z = v_2 - v_1 > 0$  means that  $v_2 > v_1$  and two particles cannot collide if the upper one moves faster upward. Hence we can state:  $(h, z) \in \mathcal{M}_1 \Rightarrow z < 0$ .

Consider the coordinates of  $D F_1 \cdot \underline{x}$  and notice that  $xy < 0 \Leftrightarrow \underline{x} \in A$ . By checking the signs of each term in the sum one can easily see that  $D F_1 \cdot \underline{x} \in A$ . In the same way  $D F_2 \cdot \underline{x} \in A$  can be derived also.

$$D F_2 \cdot \underline{x} = \begin{pmatrix} x \\ y - \frac{\sqrt{2}x}{\sqrt{hm}} \end{pmatrix}$$

We can use these cones to approximate the unstable manifolds. Take an invariant cone field and apply  $T$  to the cones (in the above mentioned way) several times.

$$T(x, v) = \begin{cases} (F_1(x), D F_1 \cdot v) & \text{if } x \in \mathcal{M}_1 \\ (F_2(x), D F_2 \cdot v) & \text{if } x \in \mathcal{M}_2 \end{cases}$$

As  $n \rightarrow \infty$  the image of the cones are getting more and more narrow (because they are mapped inside themselves, and expand also) and the limit gives the direction of the unstable subspace in every point. More precisely, to get the unstable direction of a point  $x$  one has to determine  $\lim_{n \rightarrow \infty} D T^n (\mathcal{C}_{T^{-n}x})$ . To get an approximate direction count:  $D T^N (\mathcal{C}_{T^{-N}x})$  for a sufficiently large  $N$  which gives a very narrow cone around  $\mathcal{E}_x^u$ .

The only problem is when the cones are not mapped strictly inside themselves. Considering  $D F_2 = \begin{pmatrix} 1 & 0 \\ -\sqrt{\frac{1}{2hm}} & 1 \end{pmatrix}$  we see that the cone field is invariant but

$$\begin{pmatrix} 1 & 0 \\ -\sqrt{\frac{1}{2hm}} & 1 \end{pmatrix} \cdot \begin{pmatrix} 0 \\ z \end{pmatrix} = \begin{pmatrix} 0 \\ z \end{pmatrix}$$

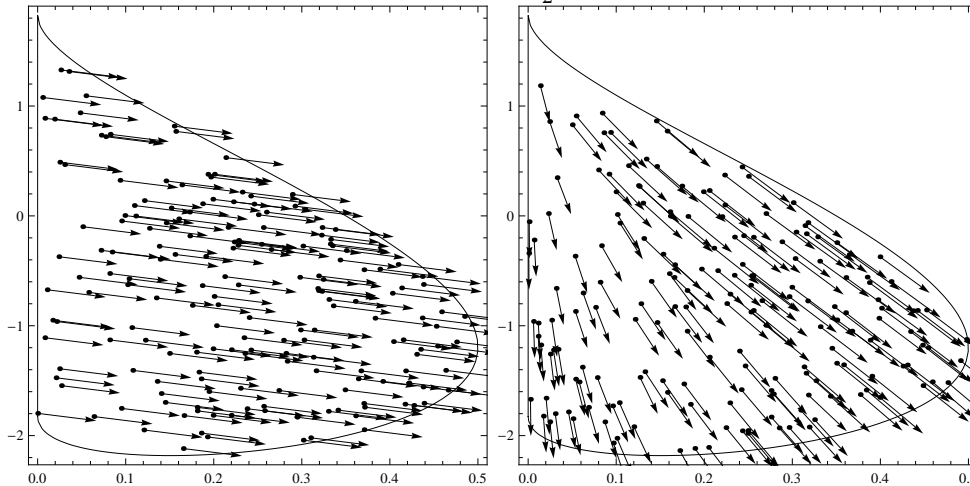
is fixed so the vertical side of the cone in  $\mathcal{M}_2$  will not narrow down.

**Definition 2.3.6** Let  $\mathcal{C}_1, \mathcal{C}_2 \subseteq A$  be two cones in a metric space. Assume that  $\mathcal{C}_1 \subseteq \mathcal{C}_2$ . We say that  $\mathcal{C}_2$  strictly contains  $\mathcal{C}_1$  ( $\mathcal{C}_1 \ll \mathcal{C}_2$ ) if:

$$\partial\mathcal{C}_2 \cap \mathcal{C}_1 = \{0\}$$

The approximation of the unstable directions requires that every cone is mapped strictly inside the cone at the image point. The cones in  $\mathcal{M}_1$  act properly since  $DF_1$  has two different eigenvalues separated from 1. The cones in  $\mathcal{M}_2$  are also mapped inside the corresponding cones but not strictly, however sooner or later any point from  $\mathcal{M}_2$  will step into  $\mathcal{M}_1$  so, eventually, every cone will narrow down properly.

Figure 2.7:  $J = \frac{1}{2}, m = 0.7$



In figure 2.7, on the left, you can see 180 randomly chosen points and a constant vector field. The vector field  $\{(x_i, (1, -1))\}_{x_i \in \mathcal{M}}$  was iterated 50 times by  $T$ , and the image is displayed on the right.

$$\left\{ \left( T^{k_0} x_i, DT_{T^{k_0} x_i} \dots DT_{T x_i} DT_{x_i} (1, -1) \right) \right\}_{x_i \in \mathcal{M}} \quad \text{with } k_0 = 50$$

The lengths of the vectors on the figure are not relevant because they were normalized in each step.

These were the unstable directions. To get the stable directions one has to find a backward-invariant family of cones and iterate them backwards.

## 2.4 The First Return Map and the Singularity Stripes

Dealing with cones we saw an interesting phenomenon: take a point in  $\mathcal{M}_2$ , iterate it by  $T$  and wait until it pops into  $\mathcal{M}_1$ . Physically this means that the lower ball

bounces for a while until it collides with the upper ball. This motivates defining the first return map of the set  $\mathcal{M}_1$  in a standard way:

$$n_* : \mathcal{M}_1 \mapsto \mathbb{N}$$

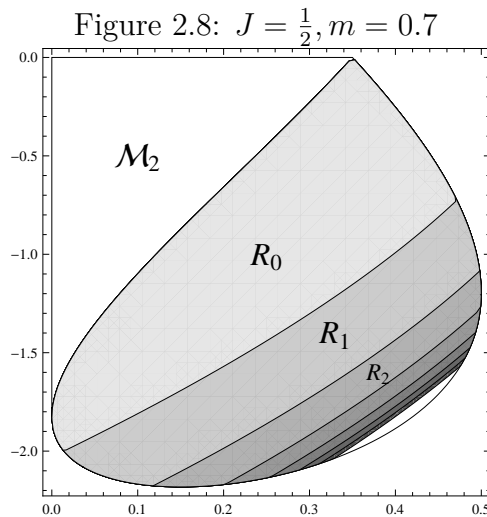
$$n_x := \min\{n \in \mathbb{N} | F_2^n(F_1(x)) \in \mathcal{M}_1\} \quad \text{the time needed to return}$$

$$R_n := \{x \in \mathcal{M}_1 | n_x = n\} \quad \text{the sets where the recurrence time is constant}$$

$$\hat{T} : \mathcal{M}_1 \mapsto \mathcal{M}_1$$

$$\hat{T}x := F_2^{n_x}(F_1(x))$$

The invariant measure for  $\hat{T}$  is the normalized Lebesgue measure on  $\mathcal{M}_1$  (a conditional probability), denoted by  $\hat{\mu}$ .



Starting from the set  $R_n$  the lower ball collides with the upper ball then hits the floor  $n + 1$  times until it collides again with the upper one. This phenomenon hastens the decay of correlations in the new system and also causes bigger rates of expansion in the Lyapunov exponents.

Notice that in the new dynamics the  $F_1$  acts on every point therefore *there are no neutral steps*, when the matrix  $D\hat{T}$  does not stretch a vector. This is called uniform hyperbolicity.

One can recalculate the exponent of the system with the new derivative matrices. Notice that  $\hat{T}$  is also piecewise continuous but with countable many singularities.

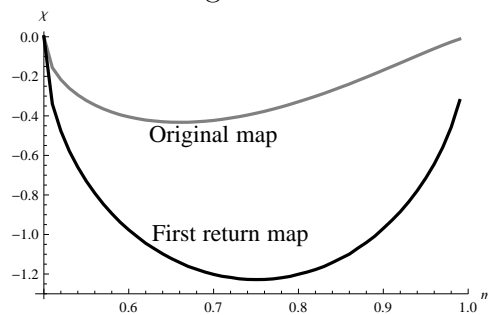
$$\begin{aligned} D\hat{T}|_{R_n} &= D(F_1 \circ \underbrace{F_2 \circ \dots \circ F_2}_{n \text{ times}}) = \\ &= D F_1 \cdot \underbrace{D F_2 \cdot \dots \cdot D F_2}_{n \text{ times}} = D F_1 \cdot D F_2^n \end{aligned}$$

The new Lyapunov exponent can be calculated in the following way:

$$\hat{\chi} = \int_{\mathcal{M}_1} \log |\text{eig}(D_x \hat{T})| d\hat{\mu}(x) = \frac{1}{\lambda(\mathcal{M}_1)} \sum_{n=0}^{\infty} \int_{R_n} \log |\text{eig}(D F_1 \cdot D F_2^n)| dh dz$$

Like in the end of section 2.3 I calculated this integral numerically. I divided the bounding rectangle of  $\mathcal{M}_1$  in  $100 \times 100$  parts, equidistantly and calculated the Riemann sum over this partition. Figure 2.9 displays the result.

Figure 2.9:



# Chapter 3

## Analysis of the First Return Sets

A long term aim of our study is to prove polynomial rate of mixing for the falling ball model. In such a proof the analysis of the sets  $R_n$  plays an important role. In [6] Chernov and Zhang discuss a general method which allows to prove decay of correlations with polynomial rate in hyperbolic systems. Their work is partly based on the results of Young ([17], [18]).

Let  $T : \mathcal{M} \mapsto \mathcal{M}$  be a mixing, non-uniformly hyperbolic dynamics with absolutely continuous invariant measure  $\mu$ . Also, let  $\mathcal{M}_1 \subseteq \mathcal{M}$  be a subset such that the first return map  $\hat{T} : \mathcal{M}_1 \mapsto \mathcal{M}_1$  is uniformly hyperbolic. Let  $R(x, T, \mathcal{M}_1)$  denote the time when the point  $x \in \mathcal{M}$  reaches the set  $\mathcal{M}_1 \subseteq \mathcal{M}$  at the first time by the dynamics  $T$ .

$$R(x, T, \mathcal{M}_1) = \min \{i \geq 1 : T^i x \in \mathcal{M}_1\}$$

Similarly,  $R$  can denote hitting times for other maps and other sets.

The main ingredient of the method is the existence of a horseshoe-like set  $\Delta_0 \subseteq \mathcal{M}_1$ , which contains stable and unstable manifolds and has a Cantor structure. Either by means of  $T$  or  $\hat{T}$ , returns to  $\Delta_0$  are always understood in a Markov-sense. This roughly means that  $\Delta_0$  can be partitioned into subsets  $\Delta_{0,i}$  that extend  $\Delta_0$  along the stable direction, the points of  $\Delta_{0,i}$  return simultaneously, and when they return, they extend  $\Delta_0$  along the unstable direction. The speed of mixing is highly correlated with the return times. Young in [17] proved that if the distribution  $\mu \{x \in \mathcal{M} | R(x, \Delta_0, \hat{T}) > n\}$  has an exponential tail bound, then the map  $\hat{T}$  enjoys exponential decay of correlations. Later in [18] she proved that the polynomial tail bound implies polynomial mixing rate.

Let us consider first the uniformly hyperbolic map  $\hat{T} : \mathcal{M}_1 \mapsto \mathcal{M}_1$ . Chernov and Zhang formulated in [6] a set of conditions which guarantee the existence of  $\Delta_0$  and exponential tail bound for  $R(x, \Delta_0, \hat{T})$  (hence exponential decay of correlations for  $\hat{T}$ ). Beside uniform hyperbolicity the essence is a Growth Lemma-like condition

about the expansion rates of the unstable manifolds.

Now let us consider the original map  $T : \mathcal{M} \mapsto \mathcal{M}$ . If we have a  $\Delta_0$  in the set  $\mathcal{M}_1 \subseteq \mathcal{M}$  which satisfies the conditions above, then we hope that, beside the first return map, the original map also enjoys decay of correlations, however with a slower rate (based on [18]). Chernov and Zhang proved that the same  $\Delta_0$  also satisfies a (slower) tail bound for the return times by the original dynamics if the return times of the first return map satisfies a polynomial tail bound. Precisely: if the set  $\Delta_0 \subseteq \mathcal{M}_1$  satisfies that

$$\begin{aligned} \mu(x \in \mathcal{M}_1 | R(x, \Delta_0, \hat{T}) > n) &\leq \text{const } \theta^n \quad (\text{for some } \theta < 1) \quad \text{and we know that} \\ \mu(x \in \mathcal{M}_1 | R(x, \mathcal{M}_1, T) > n) &\leq \text{const } n^{-a-1} \quad (\text{for some } a > 0) \quad \text{then} \\ \mu(x \in \mathcal{M} | R(x, \Delta_0, T) > n) &\leq \text{const } \log n^{a+1} n^{-a} \end{aligned}$$

And this tail bound implies the decay of correlations for the original dynamics  $T : \mathcal{M} \mapsto \mathcal{M}$ .

Summarizing, if we have an ergodic and non-uniformly hyperbolic dynamics  $T : \mathcal{M} \mapsto \mathcal{M}$  and we can localize a set  $\mathcal{M}_1 \subseteq \mathcal{M}$  where the first return dynamics  $\hat{T} : \mathcal{M}_1 \mapsto \mathcal{M}_1$  is uniformly hyperbolic, then the exponential mixing rate of  $\hat{T}$  and the polynomial tail bound for the return times implies the polynomial mixing rate in the original dynamics.

I will not consider the existence of the  $\Delta_0$  but it seems possible to verify the conditions of Chernov and Zhang by the study of the asymptotic behaviour of the eigenvalues of  $D F_1$  and  $D F_2$ . It is a long term project to complete this proof after this thesis. Now I will prove only that

$$\mu(x \in \mathcal{M}_1 | R(x, T, \mathcal{M}_1) > n) \leq \text{const } n^{-a-1} \quad \forall n \geq 1 \quad (3.1)$$

For some  $a > 0$  constant. This condition (with the existence of the  $\Delta_0 \subseteq \mathcal{M}_1$ ) would imply the following for Hölder continuous observables  $f$  and  $g$ .

$$|\mathbb{E}((f \circ T^n)g) - \mathbb{E}(f)\mathbb{E}(g)| \leq \text{const} \cdot (\log n)^{a+1} n^{-a} \quad \forall n \geq 1 \quad (3.2)$$

Condition 3.1, applied to our system, requires to find two constants,  $a > 2$  and a  $c > 0$  (which may depend on the mass ratio  $m$ ) such that

$$\mu(R_n) \leq c n^{-a} \quad \forall n \geq 1.$$

### 3.1 Bounding Functions

To estimate the measure of  $R_n$  I determined the curves bounding these sets. The curve that defines the boundary of the whole  $\mathcal{M}$  can be derived by solving the

equation:

$$J - h = \frac{1}{2}m_2v_2^2$$

$$J - h = \frac{1}{2}(1 - m) \left( \sqrt{\frac{2h}{m}} + z \right)^2$$

In section 2.1 we defined  $\mathcal{M}$  via this quantity. Solving it for  $h$  defines a function  $h = l_{m,J}(z)$  and solving it for  $z$  would define a function  $z = l_{m,J}(h)$ . The former one produces shorter formulas. Also assume that  $J = \frac{1}{2}$ .

$$l_m(z) = \frac{1}{2}m \left( 1 \pm 2(1 - m)z\sqrt{1 - (1 - m)mz^2} + z^2\alpha \right)$$

Since  $z < 0$  ( $(h, z) \in \mathcal{M}_1$ ) the "-" sign represents the greater quantity from the two options thus we should use "-" to get the curve that bounds  $\mathcal{M}$  from the right. See figure 3.1.

To express the curves separating the sets  $R_n$  and  $R_{n+1}$  let

$$(h'(h, z), z'(h, z)) = F_2^n(F_1(h, z))$$

and test whether  $(h', z')$  is on the boundary of  $\mathcal{M}_1$  by solving the following equation for  $h$ .

$$h_t = \frac{m_2m_1z' \left( 2\sqrt{\frac{2h'}{m_1}} - z' \right) - 2h' \overbrace{(m_1 + m_2)}^1 + \overbrace{2J}^1 m_1}{2gm_1m_2} =$$

$$\frac{(1 - m)mz' \left( 2\sqrt{\frac{2h'}{m}} - z' \right) - 2h' + m}{2gm(1 - m)} = 0$$

$$\Downarrow$$

$$(1 - m)mz' \left( 2\sqrt{\frac{2h'}{m}} - z' \right) - 2h' + m = 0$$

Where  $h_t$  is from the formula (2.1) which characterizes  $\mathcal{M}_1$ .

After the substitutions and some simplifications the equation to solve takes the following form.

$$2 \left( 1 - \frac{h}{m} + z^2\alpha \right) - 1 +$$

$$(1 - m) \left( 2\sqrt{2}(n + 1)\sqrt{1 - \frac{h}{m} + z^2\alpha} + z \right) \left( \sqrt{2}(2n + 4)\sqrt{1 - \frac{h}{m} + z^2\alpha} + z \right) = 0$$

Let  $F(h, z)$  denote the quantity  $\sqrt{1 - \frac{h}{m} + z^2\alpha}$  and solve the equation for  $F$ .

$$2F^2 - 1 + (1 - m) \left( 2\sqrt{2}(n+1)F + z \right) \left( \sqrt{2}(2n+4)F + z \right) = 0$$

$$\Downarrow$$

$$F = \frac{(1 - m)(2n + 3)z \pm \sqrt{m^2z^2 - m(4n^2 + 12n + z^2 + 8) + (2n + 3)^2}}{\sqrt{2}(4m(n^2 + 3n + 2) - (2n + 3)^2)}$$

We have to choose the non-negative solution. First consider the denominator.

$$\begin{aligned} \sqrt{2} \left( 4m(n^2 + 3n + 2) - (2n + 3)^2 \right) &< 0 \\ 4m(n^2 + 3n + 2) - (2n + 3)^2 &< 0 \\ 4m(n^2 + 3n + 2) &< (2n + 3)^2 \\ m(4n^2 + 12n + 8) &< 4n^2 + 12n + 9 \end{aligned}$$

Since  $0 < m < 1$  the denominator is negative indeed. In order to have a negative numerator take the "-" sign (notice that  $z < 0$  since every point is in  $\mathcal{M}_1$ ). Now we can solve the following equation for  $h$  to eliminate  $F$ .

$$\overbrace{1 - \frac{h}{m} + z^2\alpha}^{F^2} = \left( \frac{(1 - m)(2n + 3)z - \sqrt{m^2z^2 - m(4n^2 + 12n + z^2 + 8) + (2n + 3)^2}}{\sqrt{2}(4m(n^2 + 3n + 2) - (2n + 3)^2)} \right)^2$$

Let  $r_m^n(z)$  denote the solution, the bounding curve of  $R_n$ .

$$\begin{aligned} r_m^n(z) &:= m + mz^2\alpha - \\ &- m \left( \frac{(1 - m)(2n + 3)z - \sqrt{m^2z^2 - m(4n^2 + 12n + z^2 + 8) + (2n + 3)^2}}{\sqrt{2}(4m(n^2 + 3n + 2) - (2n + 3)^2)} \right)^2 \end{aligned} \quad (3.3)$$

Theoretically knowing these formulas would allow us to calculate the exact value of  $\mu(R_n)$ . But the integrals seem impossible to calculate. For example finding the intersection of  $r_m^n(z)$  and  $l_m(z)$  results a more than fourth order equation. Even if one could calculate the integrals the formulas were too long to treat them. My estimation is based on the asymptotic behaviour of  $r_m^n(z)$ .

## 3.2 A Simplified Model

As the figures 3.1 and 2.8 suggest, there is a limit where the functions  $r_m^n$  tend to.

$$r_m(z) := r_m^\infty(z) = \lim_{n \rightarrow \infty} r_m^n(z) = m(1 + \alpha z^2)$$



Figure 3.1:  $J = \frac{1}{2}, m = 0.6$

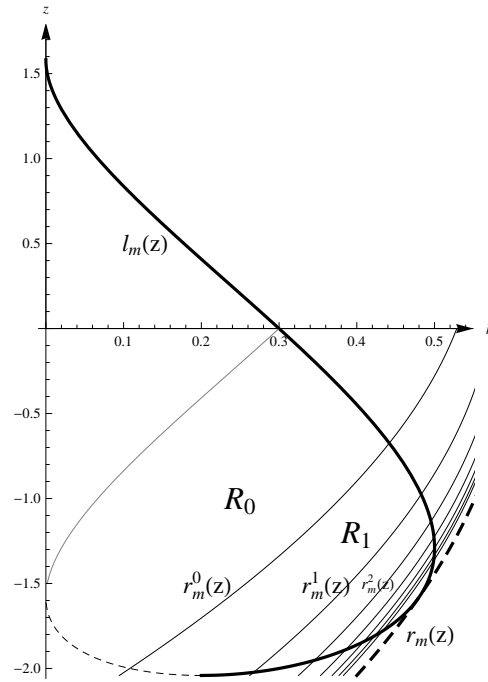
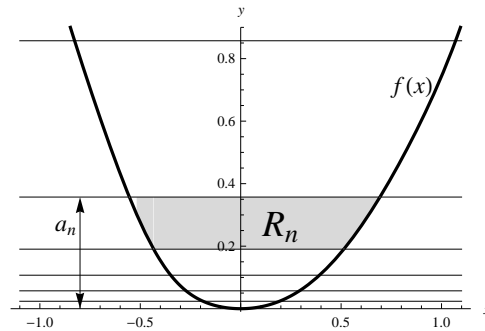


Figure 3.2: A simplified model



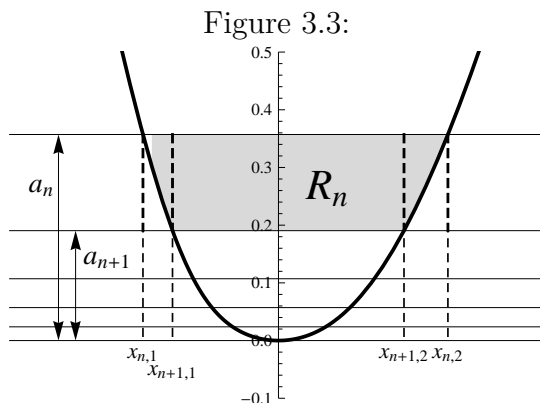
The figures also suggest that the sets  $R_n$  are shaped like parallel stripes and these stripes accumulate on  $r_m(z)$ . We can make a strongly simplified model of the stripes. Take a sequence of parallel and horizontal lines crossed by the graph of a specific function  $f(x)$ . The height of the  $n^{\text{th}}$  line is  $a_n$ .  $f(x)$  simulates  $l_m(z)$  and the  $a_n$  (constant function) is an analogue of  $r_m^n(z)$ . First we will obtain an upper bound on the areas in this simple case, and consider the relevance of this model in section 3.4.

Notice that the tail bound for  $\mu(R_n)$  is strongly determined by the order of the first non-vanishing derivative of  $f$  in 0. The higher the degree of the tangency is, the less rapidly the areas of  $R_n$  decrease. To maintain the concept of figure 3.2 we make some restrictions on  $f$ . These restrictions are stronger requirements than what is actually needed because we are interested in the behaviour of a concrete function and we do not want to formalize a general theorem. Suppose that  $f$  is continuous,

and  $f$  is monotone decreasing for  $x < 0$  and monotone increasing for  $x > 0$  (consider only a small neighbourhood of 0). Also suppose that the following limit exists.

$$\lim_{x \rightarrow 0} \frac{f(x)}{x^k} = D \quad (3.4)$$

for some even number  $k$  and  $D > 0$ . This property implies that the first  $k$  derivatives of  $f$  exist in 0 and the value of the first non-vanishing derivative is  $k! \cdot D$ . Another consequence of these properties is that  $f(0) = 0$  and  $f$  has a local minimum in 0, therefore the equation  $f(x) = a_n$  has exactly two solutions (for a sufficiently large  $n$ ):  $x_{n,1} < 0 < x_{n,2}$ .



With these notations:

$$(x_{n+1,2} - x_{n+1,1})(a_n - a_{n+1}) \leq \mu(R_n) \leq (x_{n,2} - x_{n,1})(a_n - a_{n+1})$$

Now let us estimate  $x_{n,2} - x_{n,1}$  from above.

$$\begin{aligned} f(x_{n,1}) &= a_n \\ (x_{n,1})^k \frac{f(x_{n,1})}{(x_{n,1})^k} &= a_n \end{aligned}$$

We are able to estimate the term  $\frac{f(x)}{x^k}$  since the limit (3.4) exists. There exist constants (depending on  $f$ )  $c_1, c_2$  and an  $N_0 \in \mathbb{N}$  such that  $0 < c_1 \leq D \leq c_2$  and  $c_1 \leq \frac{f(x_{n,1})}{(x_{n,1})^k} \leq c_2$  holds for  $n > N_0$  (notice that  $x_{n,1} \rightarrow 0$  as  $n \rightarrow \infty$ ).

$$\begin{aligned} (x_{n,1})^k \frac{f(x_{n,1})}{(x_{n,1})^k} &= a_n \\ (x_{n,1})^k c_1 &\leq a_n \leq (x_{n,1})^k c_2 \\ (x_{n,1})^k &\leq \frac{a_n}{c_1} \\ -x_{n,1} = |x_{n,1}| &\leq \sqrt[k]{\frac{a_n}{c_1}} \end{aligned}$$

In the same way we can estimate  $x_{n,2}$ . There exist other constants  $d_1, d_2$  and an  $M_0 \in \mathbb{N}$  such that  $0 < d_1 \leq D \leq d_2$  and  $d_1 \leq \frac{f(x_{n,2})}{(x_{n,2})^k} \leq d_2$  holds for  $n > M_0$ .

$$\begin{aligned} (x_{n,2})^k \frac{f(x_{n,2})}{(x_{n,2})^k} &= a_n \\ (x_{n,2})^k d_1 &\leq a_n \leq (x_{n,2})^k d_2 \\ (x_{n,2})^k &\leq \frac{a_n}{d_1} \\ x_{n,2} &\leq \sqrt[k]{\frac{a_n}{d_1}} \end{aligned}$$

Hence

$$\begin{aligned} \mu(R_n) &\leq (x_{n,2} - x_{n,1})(a_n - a_{n+1}) \\ \mu(R_n) &\leq \left( \sqrt[k]{\frac{a_n}{d_1}} + \sqrt[k]{\frac{a_n}{c_1}} \right) (a_n - a_{n+1}) \quad \text{if } n > \max \{N_0, M_0\} \\ \mu(R_n) &\leq \left( \sqrt[k]{\frac{1}{d_1}} + \sqrt[k]{\frac{1}{c_1}} \right) \sqrt[k]{a_n} (a_n - a_{n+1}) \quad \text{let } a_n = \frac{1}{n^\alpha} \\ \mu(R_n) &= \mathcal{O} \left( \frac{1}{n^{\frac{\alpha}{k}}} \frac{1}{n^{\alpha+1}} \right) = \boxed{\mathcal{O} \left( \frac{1}{n^{\alpha+1+\frac{\alpha}{k}}} \right)} \end{aligned} \tag{3.5}$$

Notice that the bigger the  $k$  the slower the  $\mu(R_n)$  tends to 0. It is also possible to obtain a lower bound estimation with the same argument. Even though it is not needed in our proof, in other studies, like in [2], a lower bound is necessary.

### 3.3 Straightening the Stripes

In the following section I will construct a map which distorts the plane in such a way that the graphs of the  $r_m^n(z)$  become the translated versions of the graph of  $r_m(z)$ . This is the first step to transform the  $R_n$  into the form of figure 3.2. Notice that to obtain a correct estimation I have to prove that the Jacobian of this map is uniformly bounded away from both 0 and  $\infty$ .

Let  $\pi$  denote the transformation that straightens the graphs of  $r_m^n$ . We require that  $\pi$  has the following properties (for motivation see figure 3.2 or 3.3).

$$\begin{aligned} \pi : \mathcal{R}_m &\mapsto \{(h, z) \in \mathbb{R}^2 \mid h \leq r_m(z)\} \\ \pi \begin{pmatrix} r_m^n(z) \\ z \end{pmatrix} &= \begin{pmatrix} r_m(z) - a_n \\ z \end{pmatrix} \quad \text{if } n \geq n_0(m) \end{aligned}$$

I will define  $\mathcal{R}_m$  later. In order to determine  $a_n$  let us calculate the following limits.

$$\begin{aligned}\lim_{n \rightarrow \infty} (r_m(z) - r_m^n(z)) &= 0 \quad (\text{trivially}) \\ \lim_{n \rightarrow \infty} n (r_m(z) - r_m^n(z)) &= 0 \\ \lim_{n \rightarrow \infty} n^2 (r_m(z) - r_m^n(z)) &= \frac{m \left( -(1-m)z + \sqrt{1-m} \right)^2}{8(1-m)^2} \\ \lim_{n \rightarrow \infty} n^3 (r_m(z) - r_m^n(z)) &= \infty\end{aligned}$$

I assumed that  $1 > m > 0$  and  $z < 0$  during the calculations. Suggested by this fact we make the choice  $a_n = \frac{1}{n^2}$ . At the moment  $a_n$  could be any sequence tending to 0, but this particular choice will guarantee that the transformation does not distort the area in a degenerate way, see section 3.4. We could also choose any other sequence  $a_n$  as long as  $\lim_{n \rightarrow \infty} \frac{a_n}{1/n^2} = \text{const} \neq 0, \infty$ .

One can see that  $\pi$  transforms only the  $h$  coordinate and the action of  $\pi$  depends only on  $n$ . Pretend for a while that the parameter  $n$  is continuous, as the formula of  $r_m^n$  allows to substitute  $n$  with any positive number. This kind of generalisation implies that the curves  $\{r_m^\nu(z)\}_{\nu \in [0, \infty)}$  cover the set  $\bigcup_{n \in \mathbb{N}_+} R_n$ . Moreover they cover the region  $\{(h, z) \in \mathbb{R}^2 \mid r_m^0(z) \leq h < r_m(z)\}$  (see figure 3.1). The domain of  $\pi$  will be derived from this set.

Even through the graphs  $r_m^\nu(z)$  cover the above mentioned region, they do not foliate that. To see this note that, for example,  $r_m^1(-6) = r_m^2(-6)$ , if  $m > \frac{5}{6}$ . It can be checked that the curves  $r_m^\nu(z)$  do foliate the region

$$\mathcal{R}_m := \{(h, z) \in \mathcal{M}_1 \mid z_{\min} < z < 0 \wedge r_m^{\nu_0}(z) \leq h \leq r_m(z)\}$$

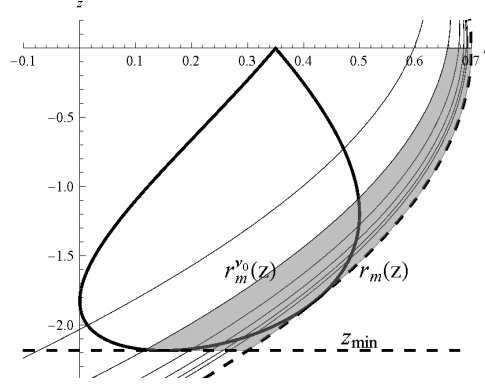
for  $\nu_0$  large enough (the value of  $\nu_0$  depends on  $m$ ).  $z_{\min}$  is the height of the lower, horizontal side of the bounding rectangle of  $\mathcal{M}_1$ . One can determine  $z_{\min}$  by checking the domain of  $l_m(z)$ .

$$\begin{aligned}l_m(z) &= \frac{1}{2}m \left( 1 - 2(1-m)z\sqrt{1 - (1-m)mz^2 + z^2\alpha} \right) \\ &1 - (1-m)mz^2 > 0 \\ z_{\min} &= \frac{-1}{\sqrt{m(1-m)}}\end{aligned}$$

Thus any point in  $\mathcal{R}_m$  can be represented with two coordinates:  $z$ , the coordinate we have already used, and the above introduced  $\nu$  which labels the graph on which  $x$  lies. To determine  $\pi$  we introduce a function which determines the  $\nu$  coordinate.

$$\begin{aligned}\nu : \mathcal{R}_m &\mapsto [0, \infty) \\ r_m^{\nu(h,z)}(z) &= h\end{aligned}$$

Figure 3.4:  $\mathcal{R}_m$



With this notation  $\pi$  can be formalized easily:

$$\pi \begin{pmatrix} h \\ z \end{pmatrix} = \begin{pmatrix} r_m(z) - \frac{1}{\nu(h,z)^2} \\ z \end{pmatrix} \quad (3.6)$$

Notice that  $\pi$  is undefined if  $\nu(h, z) = 0 \Leftrightarrow r_m^0(z) = h$ . Also one can define  $\pi$  if  $h = r_m(z) \Leftrightarrow \nu(h, z) = \infty$  in a continuous way:  $\pi(r_m(z), z) := (r_m(z), z)$ .

$$\begin{aligned} \pi : \mathcal{R}_m &\mapsto \left\{ (h, z) \in \mathbb{R}^2 \mid h \leq r_m(z) \right\} \\ \pi(h, z) &= \begin{cases} (r_m(z), z) & \text{if } \nu(h, z) = \infty \\ \left( r_m(z) - \frac{1}{\nu(h,z)^2}, z \right) & \text{otherwise} \end{cases} \end{aligned}$$

We can express the function  $\nu$  explicitly by solving the following equation (derived from (3.3)) for  $\nu$ .

$$\begin{aligned} r_m^\nu(z) &= h \\ &\Downarrow \\ \sqrt{1 - \frac{h}{m} + \alpha z^2} &= \frac{(1-m)(2\nu+3)z - \sqrt{m^2 z^2 - m(4\nu^2 + 12\nu + z^2 + 8) + (2\nu+3)^2}}{\sqrt{2}(4m(\nu^2 + 3\nu + 2) - (2\nu+3)^2)} \end{aligned}$$

This equation has two solutions, choose the positive one again. This is the function  $\nu(h, z)$ .

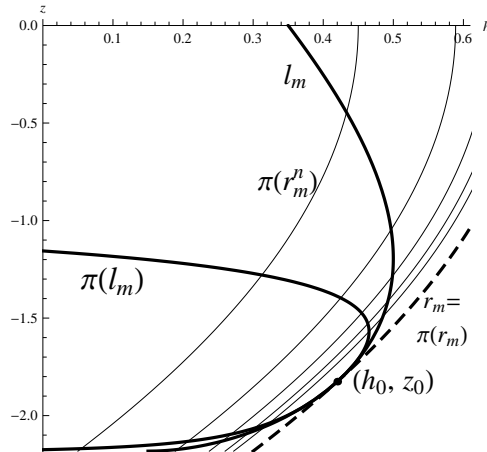
$$\nu(h, z) = \frac{\sqrt{2} \left( \sqrt{(1-m)(1-2F^2m)} - (1-m)z \right) - 6F(1-m)}{4F(1-m)}$$

Where  $F$  is a short notation for  $\sqrt{1 - \frac{h}{m} + z^2\alpha}$  as previously.

As the second step in straightening the stripes we apply a translation-like transformation.

$$\phi \begin{pmatrix} h \\ z \end{pmatrix} := \begin{pmatrix} -(h - r_m(z)) \\ z \end{pmatrix}$$

Figure 3.5: The transformed stripes

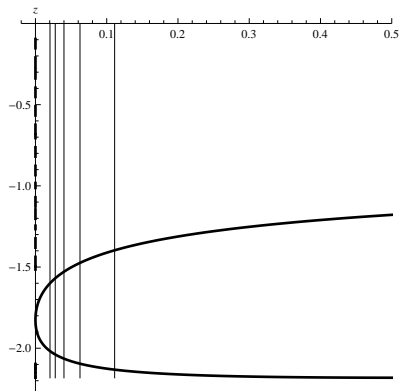


Notice that

$$\phi \left( \pi \left( \begin{pmatrix} h \\ z \end{pmatrix} \right) \right) = \begin{pmatrix} \frac{1}{\nu(h,z)^2} \\ z \end{pmatrix}$$

The transformation  $\phi \circ \pi$  distorts the figure 3.1 into the following figure.

Figure 3.6:  $\phi \circ \pi|_{\mathcal{R}_m}$



### 3.4 Summary

In the section 3.3 we constructed a transformation which maps the sets  $R_n$  into the stripes of the simplified model. Now we have to prove the non-degeneracy of the Jacobian in order to make sure that the Lebesgue measures of the sets  $R_n$  are distorted only by constant. We also have to verify that the function  $\phi(\pi(l_m(z)))$  satisfies the conditions in section 3.2, and substitute the quantities  $k$  and  $a_n$  into formula (3.5).

We do not have to prove non-degeneracy in the whole set  $\mathcal{R}_m$ , only in a neighbourhood of  $(h_0, z_0)$  since we are interested in the asymptotic behaviour of  $R_n$ . Let  $J_{h,z}$  denote the Jacobian of  $\pi$ , derived from formula (3.6). Notice that it differs

from the Jacobian of  $\phi \circ \pi$  only in it's sign, since the derivative matrix of  $\phi$  has a determinant 1.

$$J_{h,z} = \text{Det} \begin{pmatrix} \left(\frac{-1}{\nu(h,z)^2}\right)'_h & * \\ 0 & 1 \end{pmatrix} = \left(\frac{-1}{\nu(h,z)^2}\right)'_h$$

The formula of  $\left(\frac{-1}{\nu(h,z)^2}\right)'_h$  is too long to copy here. I simply calculated the following limit.

$$\lim_{h \rightarrow r_m(z)} \left(\frac{-1}{\nu(h,z)^2}\right)'_h = \frac{8(1-m)^2}{m \left(- (1-m)z + \sqrt{1-m}\right)^2}$$

This limit is non-zero and the denominator is zero if  $z = \frac{1}{\sqrt{1-m}}$ , but this point is outside of the phase space, since  $(h, z) \in \mathcal{M}_1 \Rightarrow z < 0$ . Therefore the non-degeneracy holds in a small neighbourhood of the point  $(h_0, z_0)$ . Here  $z_0$  can be calculated from the equation of  $l_m(z)$  and  $r_m(z)$ .

$$l_m(z) = r_m(z) \Rightarrow z_0 = \frac{-1}{\sqrt{1-m}}$$

To determine  $k$  we calculate the limit in formula (3.4).

$$\lim_{z \rightarrow z_0} \phi(\pi(l_m(z))) = 0 \quad (\text{trivially})$$

$$\lim_{z \rightarrow z_0} \phi(\pi(l_m(z))) (z - z_0) = 0$$

$$\lim_{z \rightarrow z_0} \phi(\pi(l_m(z))) (z - z_0)^2 = 1 - m$$

$$\lim_{z \rightarrow z_0} \phi(\pi(l_m(z))) (z - z_0)^3 = \infty$$

Hence  $k = 2$  and we can state the following.

$$\mu(R_n) \leq \text{const} \frac{1}{n^{\alpha+1+\alpha/k}} = \text{const} \frac{1}{n^{2+1+2/2}} = \text{const} \frac{1}{n^4}$$

# Chapter 4

## Afterword

In my thesis I studied the system of two falling balls. As a main result I obtained an upper bound estimation of the measures of the first return sets  $\mu(R_n)$ . I hope that this result will be a part of a complete proof in which one can state that the system enjoys polynomial decay of correlations. Following the method of Chernov and Zhang, discussed in section 3, I plan to examine the Growth Lemma-like condition by the analysis of the eigenvalues of the derivative matrices.

If the above mentioned method succeeded, then the upper bound of the decay would be  $(\log n)^3 n^{-2}$ , see formula (3.2). Since this is summable one could hope that the CLT holds too, which is another interesting direction.

I would like to thank the able help of my supervisor, Péter Bálint.



# Bibliography

- [1] V. I. Arnold, *Mathematical methods of classical mechanics*, Graduate Texts in Mathematics, 60. (1978)
- [2] Péter Bálint, Sébastien Gouëzel, *Limit theorems in the stadium billiard*, Comm. Math. Phys. **263** (2006), no. 2, 461–512.
- [3] L. Bunimovich, *Chaotic billiards* (book review), Bull. Amer. Math. Soc. (N.S.) 46 (2009), no. 4, 683–690.
- [4] N. Chernov, R. Markarian, *Introduction to the ergodic theory of chaotic billiards*, IMPA Mathematical Publications 2003
- [5] N. Chernov, *Advanced statistical properties of dispersing billiards*, Journal of Statistical Physics **122** (2006), 1061–1094.
- [6] N. Chernov, H.-K. Zhang, *Billiards with polynomial mixing rates*, Nonlinearity 18 (2005), no. 4, 1527–1553.
- [7] N. Chernov, D. Dolgopyat, *Galton Board: limit theorems and recurrence*, Journal of American Mathematical Society, **22** (2009), 821–858.
- [8] N. Chernov, G. L. Eyink, J. L. Lebowitz, Ya. G. Sinai, *Steady-state electrical conduction in the periodic Lorentz gas*, Communications in Mathematical Physics, **154** (1993), 569–601.
- [9] C. Liverani, M. P. Wojtkowski, *Ergodicity in Hamiltonian systems*, Dynamics Reported (1995), 130–202.
- [10] N. Simányi, *Conditional proof of the Boltzmann-Sinai ergodic hypothesis*, Invent. Math. 177 (2009), no. 2, 381–413.
- [11] N. Simányi, *The characteristic exponents of the falling ball model*, Comm. Math. Phys. **182** (1996), no. 2, 457–468.

- [12] Ya. Sinai, *Dynamical systems with elastic reflections. Ergodic properties of dispersing billiards*, Russian Mathematical Surveys, 25 (1970), 137–189.
- [13] Domokos Szász, *Dinamikai Rendszerek*  
  
<http://www.math.bme.hu/~szasz/eedr/dinrend.pdf>
- [14] Domokos Szász, *Boltzmann's ergodic hypothesis, a conjecture for centuries?*, Studia Sci. Math. Hungar. 31 (1996), no. 1-3, 299–322.
- [15] T. Tasnádi, *Hard Chaos in Magnetic Billiards (On the Euclidean Plane)*, Communications in Mathematical Physics, **187** (1997), 597–621.
- [16] M. P. Wojtkowski, *A system of one dimensional balls with gravity*, Comm. Math. Phys. **126** (1990), 507–533.
- [17] L.-S. Young, *Statistical properties of systems with some hyperbolicity including certain billiards*, Ann. Math., **147** (1998), 585–650.
- [18] L.-S. Young, *Recurrence times and rates of mixing*, Israel J. Math. **110** (1999), 153–188.